

Molecular Dynamics Simulations for Anisotropic Thermal Conductivity of Borophene

Yue Jia¹, Chun Li^{1,*}, Jinwu Jiang², Ning Wei³, Yang Chen⁴ and Yongjie Jessica Zhang⁵

Abstract: The present work carries out molecular dynamics simulations to compute the thermal conductivity of the borophene nanoribbon and the borophene nanotube using the Müller-Plathe approach. We investigate the thermal conductivity of the armchair and zigzag borophenes, and show the strong anisotropic thermal conductivity property of borophene. We compare results of the borophene nanoribbon and the borophene nanotube, and find the thermal conductivity of the borophene is orientation dependent. The thermal conductivity of the borophene does not vary as changing the width of the borophene nanoribbon and the perimeter of the borophene nanotube. In addition, the thermal conductivity of the borophene is not sensitive to the applied strains and the background temperatures.

Keywords: Borophene, molecular dynamics, thermal conductivity.

1 Introduction

Boron sheet is commonly named as borophene, which consists of boron atoms with 2D nanostructure. In recent years, borophene has been synthesized through experiments in several labs [Mannix, Zhou, Kiraly et al. (2015); Tai, Hu, Zhou et al. (2015); Feng, Zhang, Zhong et al. (2016)], which makes a breakthrough for the borophene research. Borophene has attracted a lot of interests in research due to its fascinating physical and chemical properties. Because of its special anisotropic crystal structure, borophene also exhibits an optical anisotropy property, which can be used as transparent conductors in display technologies, photovoltaics and flexible electronic devices [Peng, Zhang, Shao et al. (2016)]. Borophene has been found having intrinsic phonon-mediated superconductivity under estimated critical temperature when it is feasibly formed on a metal substrate [Penev,

¹ School of Mechanics, Civil Engineering and Architecture, Northwestern Polytechnical University, Xi'an, 710129, China.

² Shanghai Institute of Applied Mathematics and Mechanics, Shanghai University, Shanghai, 200433, China.

³ School of Mechanical Engineering, Jiangnan University, Wuxi, 214122, China.

⁴ College of Water Resources and Architectural Engineering, Northwest A&F University, Yangling, 712100, China.

⁵ Department of Mechanical Engineering, Carnegie Mellon University, Pittsburgh, 15213, USA.

* Corresponding Author: Chun Li. Email: lichun@nwpu.edu.cn.

Received: 30 June 2019; Accepted: 14 August 2019.

Kutana and Yakobson (2016)]. Borophene can serve as an ideal electrode material due to its high capacity and chemical stability properties [Zhang, Hu, Cheng et al. (2016)]. Flat borophene films have been found with ultra high capacities for Mg, Na or Li-ion batteries [Mortazavi, Rahaman, Ahzi et al. (2017)]. Compared to other 2D materials, borophene is hard and brittle with negative Poisson's ratio [Sun, Li and Wan (2016); Wang, Li, Gao et al. (2016)]. Borophene has been shown to have many anisotropic properties, such as special anisotropic crystal structure, highly anisotropic metallic behavior, large optical anisotropy. However, till now, there is few research conducted on the anisotropic thermal conductivity property of the borophene, which is important to realize related potential applications.

In physics, thermal conductivity describes the property of a material to conduct heat. It is worth of noting that the existing research on the thermal conductivity of borophene is based on the first principle calculations [Xiao, Cao, Ouyang et al. (2017)]. In particular, the thermal transport property of borophene is investigated through solving the Boltzmann transport equation based on the first principle calculations. Based on the first principle calculations, single-layer borophene hydride has been studied and shown with high thermal conductivities along both zigzag and armchair directions [Mortazavi, Makaremi, Shahrokhi et al. (2018)]. Up to now, detailed study on the thermal conductivity of borophene based on molecular dynamics (MD) is still lacking.

In this work, we apply the reverse nonequilibrium molecular dynamics (RNEMD) [Müller-Plathe (1997)] to investigate the thermal conductivity of borophene. Firstly, we analyze the thermal conductivity of two types of the borophene nanoribbon (BNR), namely the armchair borophene nanoribbons (ABNR) and the zigzag borophene nanoribbons (ZBNR), respectively. We calculate the thermal conductivity of BNR with different widths. Secondly, we generate the corresponding armchair borophene nanotubes (ABNT) and zigzag borophene nanotubes (ZBNT), and compute their thermal conductivity. We also compute the thermal conductivity of the borophene nanotube (BNT) with varying perimeters. In addition, we also stretch the above model along the heat flux direction, and compute the corresponding thermal conductivities. In the end, we show borophene structures have clear thermal anisotropy property.

2 Modeling and computational methods

In this work, we perform MD simulations by using the Stillinger-Weber (SW) potential [Jiang and Zhou (2017)] to describe the interaction in borophene. The nonlinear SW potential is derived from the valence force field model. The SW potential can be applied in the MD simulation of nonlinear physical or mechanical properties for borophene. For detailed discussion about the structure of the borophene and the SW potential using in the current work, we refer to Zhou et al. [Zhou and Jiang (2017)]. All the MD simulations are achieved by the Large-scale Atomic/Molecular Massively Parallel Simulator (LAMMPS) software [Plimpton (1995)], and the borophene structural visualization is obtained by the Visual Molecular Dynamics (VMD).

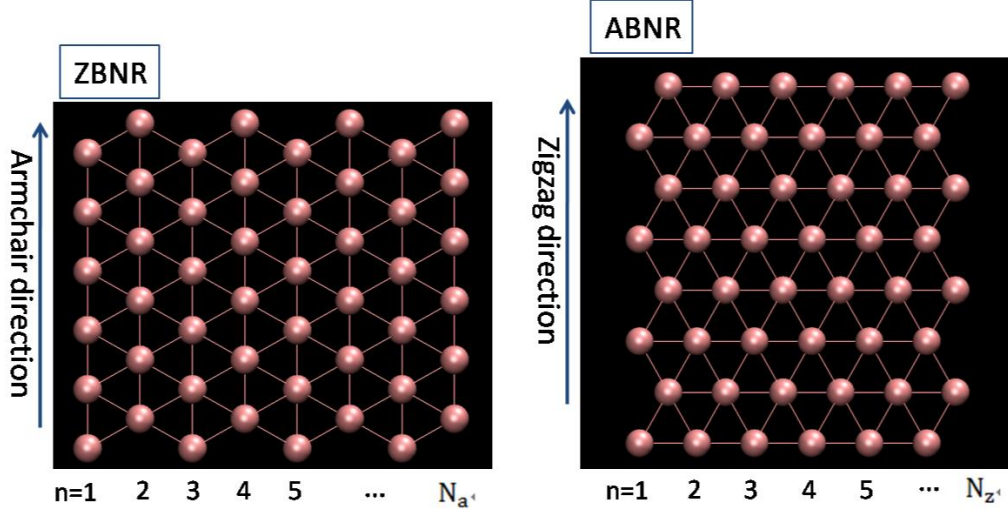


Figure 1: Atomic structure of typical armchair borophene nanoribbons (N_a -ABNR) (left) and zigzag borophene nanoribbons (N_z -ZBNR) (right). The width of BNR is labeled by the number of dimer lines, N_a for AGNR and N_z for ZBNR, respectively

Fig. 1 shows the structure of borophene (top review), in which the structural parameters are from Zhou et al. [Zhou and Jiang (2017)]. The thermal conductivity is computed by the Müller-Plathe (MP) approach [Müller-Plathe (1997)], which is one kind of RNEMD. The MP method has been successfully applied for calculating the thermal conductivity of graphene [Wei, Xu, Wang et al. (2011); Wei, Chen, Cai et al. (2016)] and phosphorene [Zhang, Pei, Jiang et al. (2016)]. Periodic boundary conditions are applied on the heat flux direction. The equilibrium temperature is given by 300 K. After 300,000 steps, the system starts the heat flux processing. The MD simulation time step is 0.5 femtosecond (fs). The simulation processing is carried out around 8,000,000 steps in total. Each period borophene nanoribbon is divided into 50 slabs along the heat transfer direction. The first slab is set to be the cold region and the 26th slab is set to be the hot region, which is shown in Fig. 2. The MP method is mainly to select the hottest atom (with the highest kinetic energy) in the cold region and the coldest atom (with the lowest kinetic energy), and pair these two atoms up and exchange their velocities. After repeating the procedure in a relatively long time, the system can reach the equilibrium state. The heat flux J is calculated by

$$J = \frac{\sum_{N_{swap}} \frac{1}{2}(mv_h^2 - mv_c^2)}{t_{swap}}, \quad (1)$$

where t_{swap} and N_{swap} are the total swap time and the number of swaps, respectively. m is the atomic mass. v_h and v_c stand for the velocities of the hottest and the coldest atoms in each time swap, respectively. The momentum exchanging is carried out every 5 fs under an NVE ensemble (constant energy and constant volume). The nonequilibrium steady state can be achieved after 100 picosecond (ps) of the exchanging process.

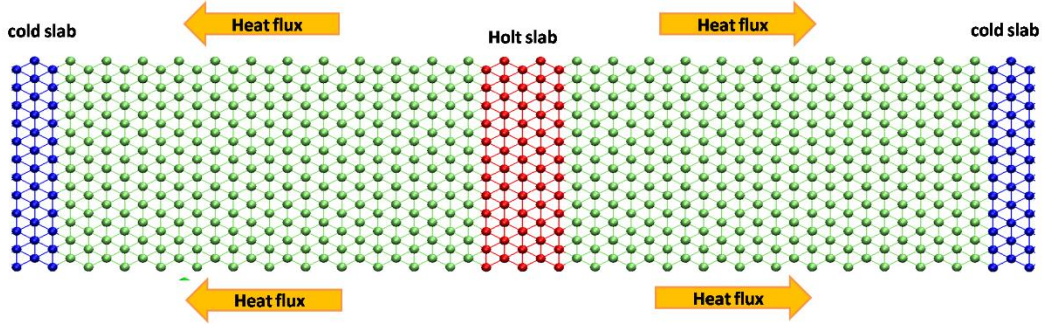


Figure 2: Schematics of the reverse non-equilibrium MD simulation

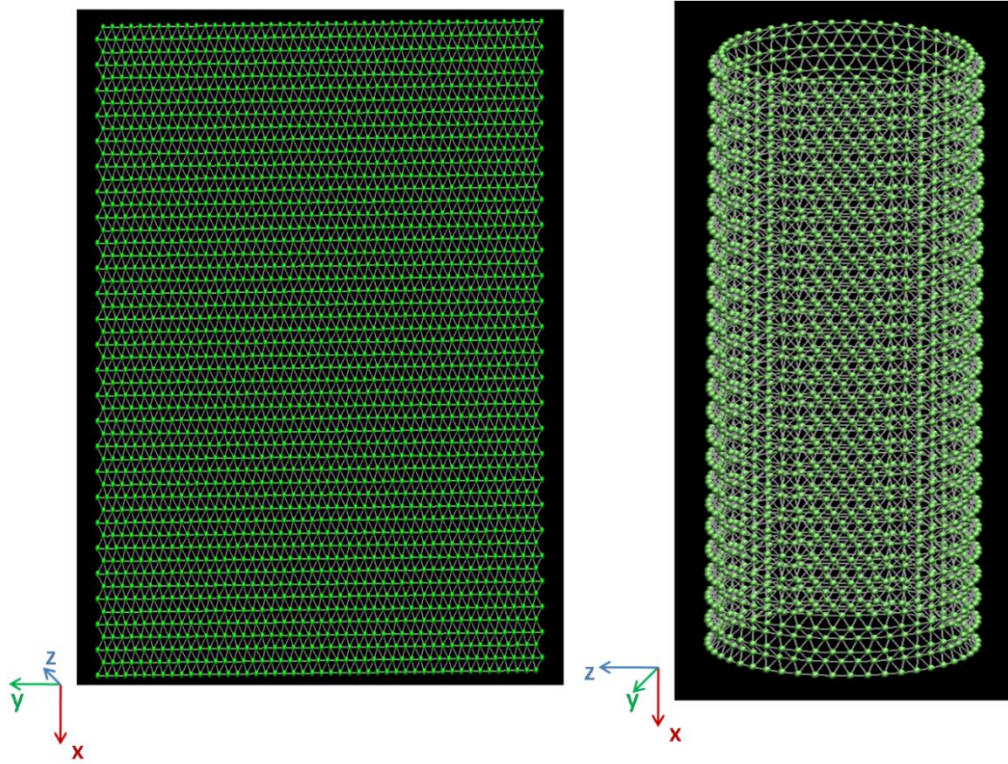


Figure 3: The configurations of the borophene nanoribbon and the borophene nanotube

The temperature distribution is collected after 10 ns (with time step 0.5 fs) and the non-equilibrium steady state is reached. The temperature of each slab is calculated from

$$T_i(\text{slab}) = \frac{2}{3Nk_B} \sum_j \frac{p_j^2}{2m}, \quad (2)$$

where $T_i(\text{slab})$ stands for the temperature of the i^{th} slab. N is the number of the boron atoms in this slab. k_B represents the Boltzmann's constant and p_j is the momentum of atom j . The temperature profiles are obtained by averaging results of around 60,000,000 steps which are collected every 30,000 steps. We show two typical

examples of temperature distribution of borophene in Fig. 4. The temperature gradient, $\frac{dT}{dx}$, can be obtained by linear fitting in the labeled region as shown in Fig. 4 (right). The thermal conductivity is obtained using the Fourier law

$$\kappa = \frac{J}{2A\partial T/\partial x} , \tag{3}$$

where A is the cross section area of the heat transfer, defined by the width multiply the thickness of the BNR. The thickness of borophene is assumed to be 0.911\AA [Zhou and Jiang (2017)], which is the distance between the top chain and the bottom chain along the out-of-plane z -direction as shown in Fig. 5.

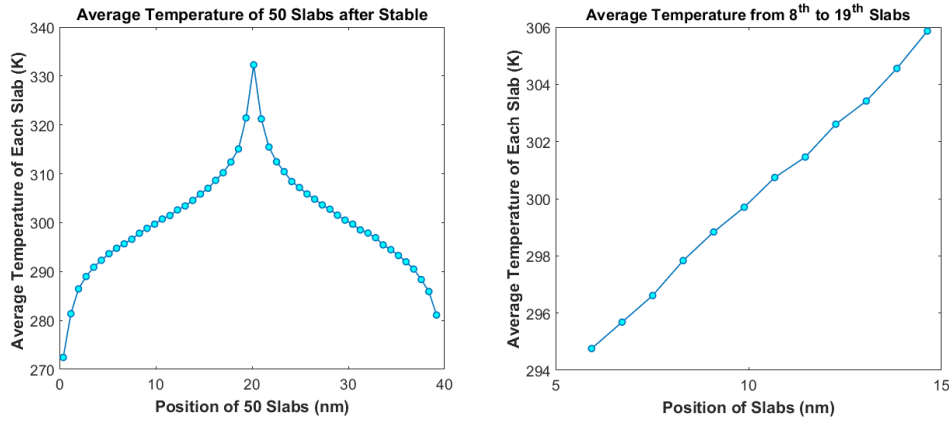


Figure 4: A typical example of temperature distribution. The temperature gradient is the function of the atom position along the x -direction which is parallel to the flux flow direction. (left) averages the temperature of each slab. (right) takes the linear segment from the temperature profile and then obtain the gradient of the segment

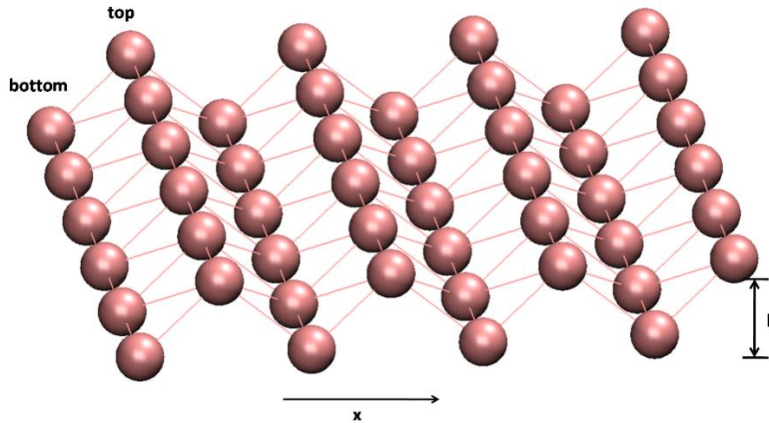


Figure 5: Perspective view illustrates the puckered configuration, with h as the distance between the top and bottom chains along the out-of-plane z -direction. The pucker is perpendicular to the x -axis and parallel with the y -axis

3 Results and discussion

3.1 Thermal conductivity of borophene nanoribbons

We first performed MD simulations to study the thermal conductivity along the armchair and zigzag directions of BNR. Simulation samples are generated with the width varying from around 10 to 30 nm, and with the same length of 40 nm. We have tested the effect of the sample width on the simulation results, and found that the thermal conductivity is width independent. From the Fig. 6, the thermal conductivity along the armchair and zigzag directions is found to be around $257.62 \text{ Wm}^{-1}\text{K}^{-1}$ and $586.12 \text{ Wm}^{-1}\text{K}^{-1}$, respectively. The borophene structures show a strong anisotropy property of the thermal conductivity. We also calculated the thermal conductivity of the BNR after applying certain amount of strain (varying from 0.5% to 2%) along the heat flux direction with varying temperatures, and the numerical results are plot in Fig. 7. However, as the strain applying of the borophene increases in different background temperatures, the corresponding thermal conductivity does not change.

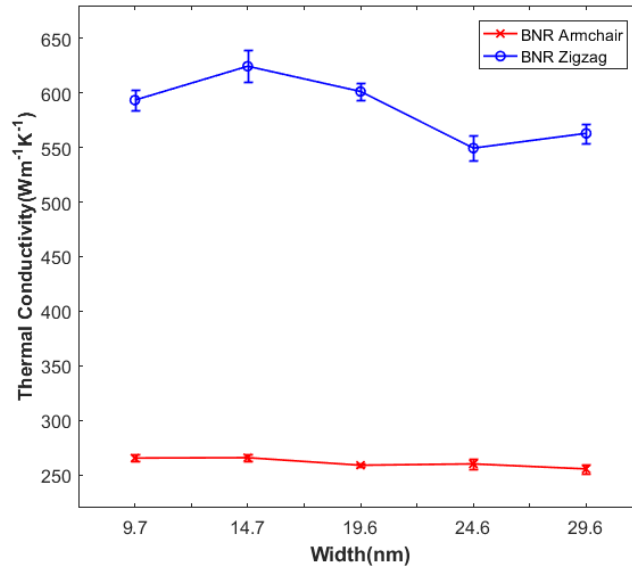


Figure 6: The calculated thermal conductivities of BNR with heat flux along the armchair direction (bottom line) and zigzag direction (above line). The length of the armchair cases is 39.551 nm, and the widths of the armchair cases are 9.684 nm, 14.526 nm, 19.852 nm, 24.694 nm and 29.536 nm. The length of the zigzag cases is 39.704 nm, and the widths of the zigzag cases are 9.744 nm, 14.903 nm, 19.489 nm, 24.648 nm and 29.806 nm

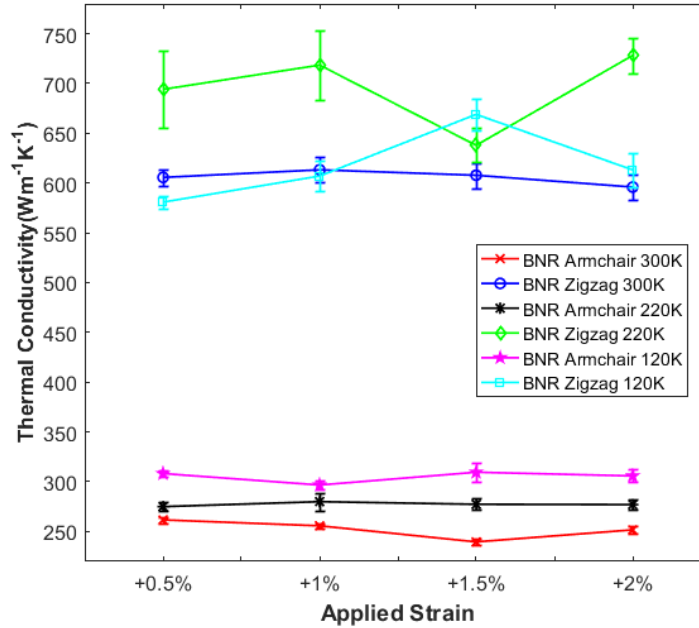


Figure 7: The calculated thermal conductivity of armchair direction BNR (bottom lines) and zigzag direction BNR (above lines) after applied strains in heat flux direction with varying temperatures. The applied strains are +0.5 %, +1%, +1.5% and +2%, respectively. The width of the armchair cases is 19.852 nm, and the lengths of the cases are 39.947 nm, 40.346 nm, 40.746 nm and 41.149 nm. The width of the zigzag cases is 19.489 nm, and the lengths of the cases are 40.102 nm, 40.502 nm, 40.904 nm and 41.308 nm

3.2 Thermal conductivity of borophene nanotubes

In order to further examine the strong thermal anisotropy property of the borophene, we generate BNT structure and apply MD to study the thermal conductivity. The in-plane thermal conductivities of the borophene along both the armchair and zigzag directions with different perimeters are showed in Fig. 8, respectively. We can observe that the thermal conductivity is around 174.86 and 408.03 $Wm^{-1}K^{-1}$ in the armchair and zigzag directions, respectively. It can be seen that the thermal conductivity of the borophene is insensitive to their perimeters. However, the comparison results show strong thermal anisotropy phenomenon for BNT as well. In order to study the strains effect of BNT, we perform MD simulations on the in-surface thermal conductivity of BNT with different strains along the heat flux direction (varying from 39.947 to 41.149 nm for the armchair type and from 40.102 to 41.308 nm for the zigzag type) in varying temperatures. From the calculated results in Fig. 9, we can observe that the thermal conductivity of BNT is not influenced by the strain and the background temperatures.

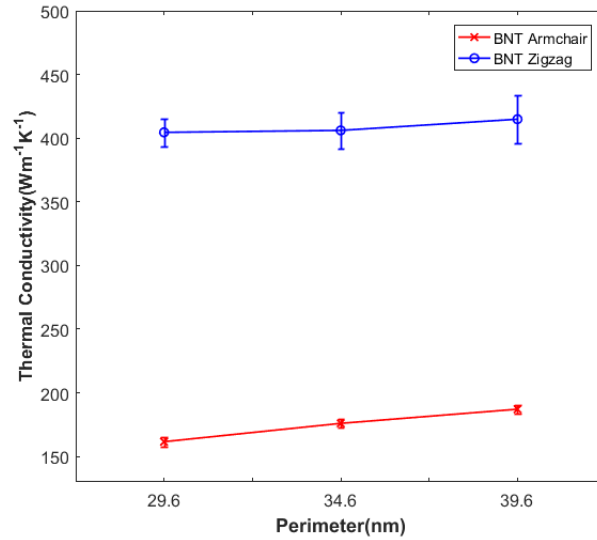


Figure 8: The calculated thermal conductivities of BNT with heat flux along the armchair direction (bottom line) and zigzag direction (above line). The length of the armchair cases is 39.551 nm, and the perimeters of the armchair cases are 29.852 nm, 34.694 nm, and 39.536 nm. The length of the zigzag cases is 39.704 nm, and the perimeters of the zigzag cases are 29.489 nm, 34.648 nm, and 39.806 nm

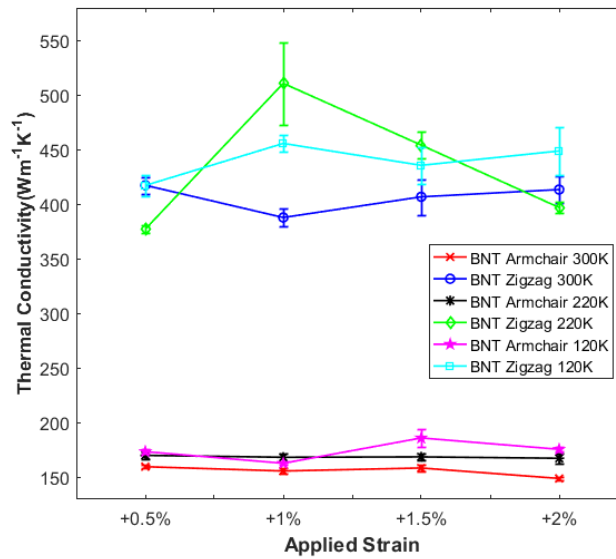


Figure 9: The calculated thermal conductivity of armchair direction BNT (bottom lines) and zigzag direction BNR (above lines) after applied strains in heat flux direction with varying temperatures. The applied strains are +0.5%, +1%, +1.5% and +2%, respectively. The perimeter of the armchair cases is 29.852 nm, and the lengths of the cases are 39.947 nm, 40.346 nm, 40.746 nm and 41.149 nm. The perimeter of the zigzag cases is 29.489 nm, and the lengths of the cases are 40.102 nm, 40.502 nm, 40.904 nm and 41.308 nm

4 Discussion

The above calculated numerical results show that borophene has strong anisotropy property for the thermal conductivity. We calculated the thermal conductivity of BNR with different widths (Fig. 6) and BNR with different perimeters (Fig. 8), and found that different widths and perimeters do not affect the thermal conductivity of the borophene. The thermal conductivity is not affected either when we stretch the BNR (Fig. 7) and BNT (Fig. 9) along the heat flux direction. If we compare the thermal conductivity of BNR (Figs. 6 and 7) with that of BNT (Figs. 8 and 9), the nanotube's is decreased. Our results show that the thermal conductivities of the borophene nanoribbon are 257.62 and 586.12 along the armchair and zigzag directions, which is inconsistent with several results based on the Reaxff potential [Mortazavi, Le, Rabczuk et al. (2017)]. It is because the thermal conductivity of the borophene is structure dependent. The differences of the thermal conductivities also happen between the borophene nanoribbon (257.62 and 586.12 along the armchair and zigzag directions) and the borophene nanotube (174.86 and 408.03 along the armchair and zigzag directions) in our current work. ReaxFF potential is accurate. However, we prefer to use the SW potential, because the SW potential considers the nonlinear effect [Jiang, Park and Rabczuk (2013)] and is rather efficient.

5 Conclusion

In this work, we use MD simulations to investigate the thermal conductivity of borophene. We calculate the thermal conductivity of BNR and BNT with the armchair and zigzag structures. We show the borophene structure has strong anisotropy property in the thermal conductivity. The thermal conductivity of the borophene with zigzag heat flux direction is much higher than that of the borophene with armchair heat flux direction. We vary the width of BNR and the perimeter of BNT, and find that the thermal conductivity of borophene is not influenced by the different widths and perimeters. After comparing the numerical results of BNR and BNT, we notice the thermal conductivity of the borophene is orientation dependent. The thermal conductivity of BNT is reduced compared to that of BNR. We also analyze the strain effect to the thermal conductivity of the borophene, which shows the thermal conductivity of borophene is insensitive to the applied strains and the background temperatures.

Acknowledgement: The authors would like to thank the support by the National NSF of China (Grant Nos. 11902263, 11572251 and 11872309), Shaanxi Science Foundation (Grant No. 2019JQ-623), and the Fundamental Research Funds for the Central Universities (Grant Nos. 310201906zy004 and 3102017jc01003). Zhang Y. was supported in part by the PECASE award N00014-16-1-2254(USA), NSF CAREER Award OCI-1149591 (USA) and NSF USA grant CBET-1804929.

Conflicts of Interest: The authors declare that they have no conflicts of interest to report regarding the present study.

References

Feng, B.; Zhang, J.; Zhong, Q.; Li, W.; Li, H. et al. (2016): Experimental realization

of two-dimensional boron sheets. *Nature Chemistry*, vol. 8, pp. 563-568.

Mannix, A. J.; Zhou, X. F.; Kiraly, B.; Wood, J. D.; Alducin, D. et al. (2015): Synthesis of borophenes: anisotropic, two-dimensional boron polymorphs. *Science*, vol. 350, no. 6267, pp. 1513-1516.

Müller-Plathe, F. (1997): A simple nonequilibrium molecular dynamics method for calculating the thermal conductivity. *Journal of Chemical Physics*, vol. 106, pp. 6082-6085.

Mortazavi, B.; Makaremi, M.; Shahrokhi, M.; Raeisi, M.; Singh, C. V. et al. (2018): Borophene hydride: a stiff 2D material with high thermal conductivity and attractive optical and electronic properties. *Nanoscale*, vol. 10, pp. 3759-3768.

Mortazavi, B.; Rahaman, O.; Ahzi, S.; Rabczuk, T. (2017): Flat borophene films as anode materials for Mg, Na or Li-ion batteries with ultra high capacities: a first-principles study. *Applied Materials Today*, vol. 8, pp. 60-67.

Mortazavi, B.; Le, M. Q.; Rabczuk, T.; Pereira, L. F. C. (2017): Anomalous strain effect on the thermal conductivity of borophene: a reactive molecular dynamics study. *Physica E*, vol. 93, pp. 202-207.

Jiang, J. W.; Zhou, Y. P. (2017): Parameterization of Stillinger-Weber potential for two-dimensional atomic crystals. arXiv:1704.03147.

Jiang, J. W.; Park, H. S.; Rabczuk, T. (2013): Molecular dynamics simulations of single-layer molybdenum disulphide (MoS₂): stillinger-Weber parametrization, mechanical properties, and thermal conductivity. *Journal of Applied Physics*, vol. 114, no. 6, 064307.

Penev, E. S.; Kutana, A.; Yakobson, B. I. (2016): Can two-dimensional boron superconduct? *Nano letters*, vol. 16, no. 4, pp. 2522-2526.

Plimpton, S. (1995): Fast parallel algorithms for short-range molecular dynamics. *Journal of Computational Physics*, vol. 117, no. 1, pp. 1-19.

Peng, B.; Zhang, H.; Shao, H.; Xu, Y.; Zhang, R. et al. (2016): Electric, optical, and thermodynamic properties of borophene from first-principle calculation. *Journal of Materials Chemistry C*, vol. 4, no. 16, pp. 3592-3598.

Sun, H.; Li, Q.; Wan, X. (2016): First-principles study of thermal properties of borophene. *Physical Chemistry Chemical Physics*, vol. 22, pp. 14927-14932.

Tai, G.; Hu, T.; Zhou, Y.; Wang, X.; Kong, J. et al. (2015): Synthesis of atomically thin boron films on copper foils. *Angewandte Chemie*, vol. 54, no. 51, pp. 15473-15477.

Wei, N.; Xu, L.; Wang, H.; Zheng, J. (2011): Strain engineering of thermal conductivity in graphene sheets and nanoribbons: a demonstration of magic flexibility. *Computers, Nanotechnology*, vol. 22, no. 10, pp. 105705.

Wei, N.; Chen, Y.; Cai, K.; Zhao, J.; Wang, H. (2016): Thermal conductivity of graphene kirigami: ultralow and strain robustness. *Carbon*, vol. 104, pp. 203-213.

Wang, H.; Li, Q.; Gao, Y.; Miao, F.; Zhou, X. et al. (2016): Strain effects on borophene: ideal strength, negative poisson's ratio and phonon instability. *New Journal of Physics*, vol. 18, pp. 73016-73022.

Xiao, H.; Cao, W.; Ouyang, T.; Guo, S.; He, C. et al. (2017): Lattice thermal

conductivity of borophene from first principle calculation. *Scientific Report*.

Zhang, X.; Hu, J.; Cheng, Y.; Yang, H.; Yao, Y. et al. (2016): Borophene as an extremely high capacity electrode material for Li-ion and Na-ion batteries. *Nanoscale*, vol. 8, no. 33, pp. 15340-15347.

Zhou, Y. P.; Jiang, J. W. (2017): Molecular dynamics simulations for mechanical properties of borophene: parameterization of valence force field model and Stillinger-Weber potential. *Scientific Report*.

Zhang, Y. Y.; Pei, Q. X.; Jiang, J. W.; Wei, N.; Zhang, Y. (2016): Thermal conductivities of single-and multi-layer phosphorene: a molecular dynamics study. *Nanoscale*, vol. 8, no. 1, pp. 483-491.